IEEE Access
Multidisciplinary | Rapid Review | Open Access Journal

Received February 26, 2019, accepted April 23, 2019, date of publication April 30, 2019, date of current version May 15, 2019.

Digital Object Identifier 10.1109/ACCESS.2019.2914064

A Novel Adaptive EEMD Method for Switchgear Partial Discharge Signal Denoising

TAO JIN[1,2], (Member, IEEE), QIANGGUANG LI[1,2], AND MOHAMED A. MOHAMED[2,3], (Member, IEEE)

[1]Fujian Key Laboratory of New Energy Generation and Power Conversion, Fuzhou 350116, China
[2]Department of Electrical Engineering, Fuzhou University, Fuzhou 350116, China
[3]Electrical Engineering Department, Faculty of Engineering, Minia University, Minia 61519, Egypt

Corresponding authors: Tao Jin (jintly@fzu.edu.cn) and Mohamed A. Mohamed (dr.mohamed.abdelaziz@mu.edu.eg)

This work was supported by the Fuzhou Municipal Science and Technology Bureau Project of China under Grant 82318048.

ABSTRACT The elimination of a variety of noises such as the narrow-band interference in the detection of partial discharge (PD) signals in switchgear is an intractable issue. Furthermore, the self-adaptation in the denoising process is weak. A partial discharge-based novel adaptive ensemble empirical mode decomposition (Novel Adaptive EEMD, NAEEMD) method is proposed in this paper for noise reduction. First, the signal is decomposed using the EEMD, only the first-order natural mode is decomposed until the signal margin reaches the EEMD decomposed termination condition. After removing the first-order mode, noise is added to the residual signal, and the remaining signal components are decomposed in the next stage. At last, the intrinsic mode function (IMF) of the noise reduction reconstruction is adaptively selected. The latter is accomplished by combining the energy density and the average period of the IMF correlation coefficient method. Meanwhile, the proposed method provides a new strategy for pre-processing the PD signal of the switchgear. The outcomes of the proposed NAEEMD de-noising method have been compared with the conventional wavelet denoising algorithm (WDA) and EMD-based threshold denoising for validation. The simulation results showed a good denoising effect and effectiveness of the proposed method compared to the WDA and EMD-based threshold denoising. Furthermore, an experimental simulation utilizing actual switchgear PD signal has been performed to verify the noise reduction effectiveness of the proposed method.

INDEX TERMS Switchgear, partial discharge, NAEEMD, narrow-band interference, denoising, wavelet transform.

I. INTRODUCTION

Nowadays, the on-line monitoring of the substation equipment is the most concerned technical field of the electric power section. Switch cabinet is a very important electrical equipment in the power system has to be monitored. The on-line monitoring of the partial discharge (PD) signal of the switch cabinet can well reflect the insulation level of the power equipment [1], [2]. But, due to the workplace factors around the switching cabinet, there is often a large number of periodic interference signals of narrow-band high frequency, in the process of obtaining PD signals. These signals are particularly random signals such as white noise. Moreover, the PD signal is a nonlinear and unstable discharge signal. Hence, how to accurately extract PD signals from noise-contaminated signals has become the key to online monitoring of PD [3], [4]. Several methods have been presented for PD signals denoising include fast Fourier transform (FFT) [5], [6], wavelet threshold denoising [7], [8] and other methods [9]–[11]. Although these methods have made great accomplishments regarding denoising, they still have few drawbacks [12]–[15]. As an example, FFT is mainly used for stationary signal denoising and the processing of non-stationary signals for PD is often not applicable [16]. Also, diverse signals are identified with human experience in selecting wavelet basis functions so that denoising effect does not always achieve people's expectations, and the uncertainty is strong. Furthermore, the denoising of wavelet threshold is not adaptive [17].

The time-frequency analysis methods of PD signal denoising include linear time-frequency analysis, adaptive time-frequency analysis and quadratic time-frequency analysis

The associate editor coordinating the review of this manuscript and approving it for publication was Ramesh Babu N.

based on Cohen's class distribution [18]–[20]. The linear time-frequency analyses such as short-time Fourier transform (STFT), Gabor transform (GT) and wavelet transform (WT). The window functions of STFT and GT are fixed and due to the limitations of their algorithms, the resolution of time domain and frequency domain cannot be optimized at the same time [21], [22]. WT can automatically adjust the time-frequency window as per the signal frequency change. As it were, it can make the resolution of time and frequency domain reach the optimal at the same time to some extent [23]. The physical significance of time-frequency distribution of Cohen's class is the distribution of signal energy in the time-domain and frequency-domain. Likewise, it can consider the overall appearance and localization qualities of time-domain and frequency-domain, yet there is a cross-term interference problem.

The Empirical Mode Decomposition (EMD) algorithm has good time-frequency characteristics, can manage nonlinear, non-stationary signals, and has strong adaptability [24]. It has accomplished important achievements in signal denoising [25], [26]. However, it is unfavorable for signal denoising analysis because of its serious modal aliasing. In order to overcome this problem, Zhu *et al.* [27] proposed the Ensemble Empirical Mode Decomposition (EEMD) method to superimpose the finite amplitude white noise multiple times in the original signal. This method makes the signal continuous on different scales to eliminate the modal aliasing phenomenon to a large extent. The idea of noise-assisted thinking method depends on the investigation of the statistical properties of white noise. But, the complexity and computational multifaceted of this method are enormously increased with expansion of white noise multiple times.

In order to overcome the above problems, a Novel Adaptive Ensemble Empirical Mode Decomposition (NAEEMD) method is proposed in this paper. Combined with the correlation coefficient method of the intrinsic mode function (IMF) of energy density and average period, the intrinsic modulus component of noise reduction reconstruction is adaptively selected. A PD signal simulation example is presented for validation and the measured signal case of the switchgear is verified. Furthermore, the wavelet adaptive threshold (WAT) denoising algorithm is compared with the threshold denoising based EMD algorithm, in terms of signal-to-noise ratio (SNR), waveform correlation (NCC), and the root mean square error (RMSE) for quantitatively comparative analysis [28], [29].

II. EEMD OF ADAPTIVE NOISE

A. NAEEMD ALGORITHM

In perspective of the drawbacks of the EEMD method, this paper proposed the NAEEMD method. The core idea of this method is that after adding white noise to the original signal, only the first-order mode is decomposed, and afterward the noise is ceaselessly added to the residual signal after the first-order mode is expelled. The next decomposition of the residual signal component, only the first-order mode is decomposed during the decomposition. Therefore, the margin of the noise adaptive EEMD method isn't gotten by independent decomposition after every addition of noise, but by the margin of the last decomposition. So as to recognize it from EEMD, the IMF component acquired by NAEEMD is recorded as c_j [30], [31]. The flowchart of NAEEMD algorithm is shown in Fig.1.

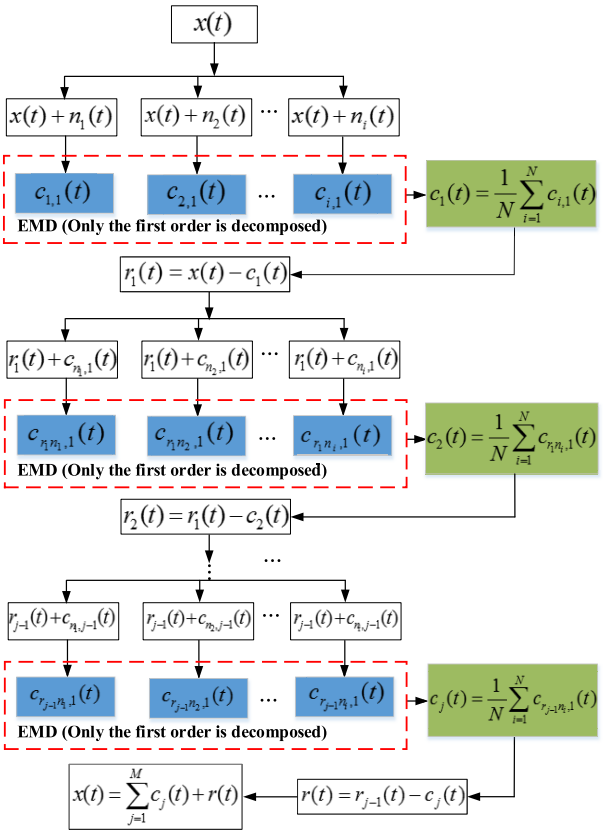

FIGURE 1. The flowchart of NAEEMD algorithm.

The specific steps of the NAEEMD algorithm are detailed as follows:

Step#1: The input signal (i.e. the original signal, $x(t)$) decides the number of times that the noise is added, N, and ε is the amplitude coefficient of the added noise.

Step#2: Adding white noise to the original signal $x(t)$ as the following:

$$x_i(t) = x(t) + n_i(t) \tag{1}$$

where $n_i(t)$ is the white noise sequence added for the $i-th$ time, $x_i(t)$ is the noise-absorbing signal.

Step#3: EMD decomposition of the signal $x_i(t)$, only the first-order mode $c_{i,1}$ is decomposed at a time, the result is as follows [32], [33]:

$$c_1(t) = \frac{1}{N}\sum_{i=1}^{N} c_{i,1}(t) \tag{2}$$

where N is the number of times of Gaussian white noise, $c_1(t)$ is the first order IMF component of NAEEMD decomposition, and $c_{i,1}(t)$ is the first order IMF component of NAEEMD decomposition after the i addition of Gaussian white noise.

Step#4: Calculation the decomposition $r_1(t)$ to get the margin after the first order mode $c_1(t)$ as follows:

$$r_1(t) = x(t) - c_1(t) \tag{3}$$

Step#5: Decomposition for each added Gaussian white noise $n_i(t)$, $i = 1, 2, \ldots N$ as the following:

$$N_i(t) = \begin{pmatrix} n_1(t) \\ n_2(t) \\ \cdots \\ n_i(t) \end{pmatrix} \overset{EMD}{\rightarrow} \begin{pmatrix} c_{n_1,1}(t) & c_{n_1,2}(t) & \ldots & c_{n_1,j}(t) & r_{n_1}(t) \\ c_{n_2,1}(t) & c_{n_2,2}(t) & \ldots & c_{n_2,j}(t) & r_{n_2}(t) \\ \cdots & \cdots & \cdots & \cdots & \cdots \\ c_{n_i,1}(t) & c_{n_i,2}(t) & \ldots & c_{n_i,j}(t) & r_{n_i}(t) \end{pmatrix} \tag{4}$$

where $c_{n_i,j}(t)$ is the $j-th$ order IMF component obtained by decomposing noise $n_i(t)$, $r_{n_i}(t)$ is the margin obtained by decomposing the noise $n_i(t)$.

At the same time, a function $D_j(x_i(t))$ is defined, that represents a set of $j-th$ order IMF after the EMD decomposition of the signal as follows [34]:

$$D_1(n_i(t)) = \begin{pmatrix} c_{n_1,1}(t) & c_{n_2,1}(t) & \ldots & c_{n_i,1}(t) \end{pmatrix}^T \tag{5}$$

where T is the matrix transpose.

Step#6: Construct a new signal $x_{new_1}(t) = r_1(t) + D_1(n_i(t))$ for next decomposition as the following:

$$x_{nar_1}(t) = r_1(t) + \begin{pmatrix} c_{n_1,1}(t) \\ c_{n_2,1}(t) \\ \cdots \\ c_{n_i,1}(t) \end{pmatrix} \xrightarrow{\text{EMD (Only lecomposes the first order 1}} \begin{pmatrix} c_{r_1 n_1,1}(t) \\ c_{r_1 n_2,1}(t) \\ c_{r_1 n_2,1}(t) \\ \cdots \\ c_{r_1 n_i,1}(t) \end{pmatrix} \tag{6}$$

where $c_{r_1 n_i,1}(t)$ is the first order IMF component decomposition after the addition of $D_1(n_i(t))$.

Step#7: Acquiring the second-order IMF component $c_2(t)$ and margin $r_2(t)$ obtained by the NAEEMD algorithm as the following.

$$c_2(t) = \frac{1}{N} \sum_{i=1}^{N} c_{r_1 n_i,1}(t) \tag{7}$$

$$r_2(t) = r_1(t) - c_2(t) \tag{8}$$

Step#8: Determine the $j-th$ order IMF of the original signal, construct a new signal and repeat Step#4 and Step#5 as follows:

$$x_{new_{j-1}}(t) = r_{j-1}(t) + D_{j-1}(n_i(t)) \tag{9}$$

$$c_j(t) = \frac{1}{N} \sum_{i=1}^{N} c_{r_{j-1} n_i,1}(t) \tag{10}$$

The final margin $r(t)$ is:

$$r(t) = x(t) - \sum_{j=1}^{M} c_j(t) \tag{11}$$

It tends to be seen from equations (1) to (11) that the NAEEMD algorithm makes smart utilization of the uniform conveyance of the white noise spectrum. So that the signal can be projected on a white noise background spread over the whole time-frequency space and chose in order to diminish the modal aliasing phenomenon. In addition, unlike EEMD algorithm, the margin of NAEEMD doesn't rely on the independent decomposition after every addition of noise, yet relies on the margin of the last decomposition, which in turn diminishes the reconstruction error after decomposition.

B. SIGNAL RECONSTRUCTION BASED-CORRELATION COEFFICIENT METHOD

The essential thought of denoising of NAEEMD algorithm is to decompose the original signal into a series of IMF components arranged in orders of frequencies from high to low. At that point, specify whether each order of IMF is a noise or a signal through some corresponding noise assessment criterias. The noise component is eliminated, and the remaining IMF component is recombined to acquire a noise-reduced signal. The commonly used IMF decision criteria includes correlation analysis method, mutual information value, adjacent signal standard deviation, continuous mean square error, etc. [35], [36]. In this paper an IMF correlation coefficient method based on energy density and average period is proposed to choose the reconstructed IMF component.

By using the EEMD noise adaptive algorithm, the energy density, E_j and the averaging period of the $j-th$ order IMF, T_j can be calculated, respectively as the following:

$$E_j = \frac{1}{N} \sum_{i=1}^{N} \left[c_j(i)\right]^2 \tag{12}$$

$$T_j = \frac{2N}{g_j} \tag{13}$$

where N is the length of each order of IMF and g_j is the number of extreme points of the $j-th$ order IMF c_j.

Based on the conclusion in [37], the product of the energy density of each order IMF component obtained by decomposition of the white noise sequence and its average period is a constant, namely:

$$S_j = E_j T_j = const \tag{14}$$

Then, the IMF correlation coefficient, RS_j which depends on the energy density and average period is defined as [38]:

$$RS_j = \left| \frac{S_j}{S_{j-1}} \right| = \left| \frac{S_j}{\frac{1}{j-1} \sum_{i=1}^{j-1} S_i} \right| \tag{15}$$

where S_j is the product of the energy density of the $j-th$ order IMF and the averaging period, S_{j-1} is the mean of the product of the energy density of the $(1 \sim j\text{-}1)th$ order IMF and the average period.

When $RS_j > 1$, it can be seen that the $j-th$ order IMF S_j is larger than the former $(j\text{-}1)th$ IMF S_{j-1}, indicating that the product of the energy density of each order IMF and its average period is constant in the $(j\text{-}1)th$ IMFs. Therefore, the former $(j\text{-}1)th$ IMF is the noise component and is rejected during reconstructing the signal. This method can effectively distinguish the noise component and avoid the denoising effect of the algorithm due to improper selection of the truncation order of the IMF components [39].

III. SIMULATION EXAMPLE

The attenuated PD signal can be theoretically analyzed by the double exponential oscillation attenuation model. Assuming the following pulse signal [40]:

$$f(t) = A(e^{-1.3t/\tau} - e^{-2.2t/\tau}) \sin(2\pi f_c t) \tag{16}$$

where A is the partial amplitude of the pulse signal, τ is the attenuation coefficient, f_c is the oscillation frequency and the sampling frequency is $f = 10$MHz. The added white noise interference signal is $w \sim N(0, 0.2^2)$. The mathematical expression of the narrowband periodic interference signal is as the following:

$$f_i(t) = \sum_{i=1}^{4} A_i \sin(2\pi f_i t) \tag{17}$$

where A_i is the amplitude of narrowband periodic interference signal, and f_i is the frequency. The PD simulation parameters are shown in Table 1.

TABLE 1. The PD simulation model parameters.

A / V	τ / μs	f_c / MHz	A_i / V	f_i / MHz
8	2.5	2	0.5	0.05
10	2	2	1	0.05
9	3	3	0.5	0.1
12	4	3	2	1

The simulated PD signal, the noise-diffused signal under narrow-band periodic interference and the white noise interference are shown in Fig.2. Figure 2(a) shows the analog PD signal, and Fig.2(b) shows the noise signal after adding the narrowband interference and the white noise. The NAEEMD

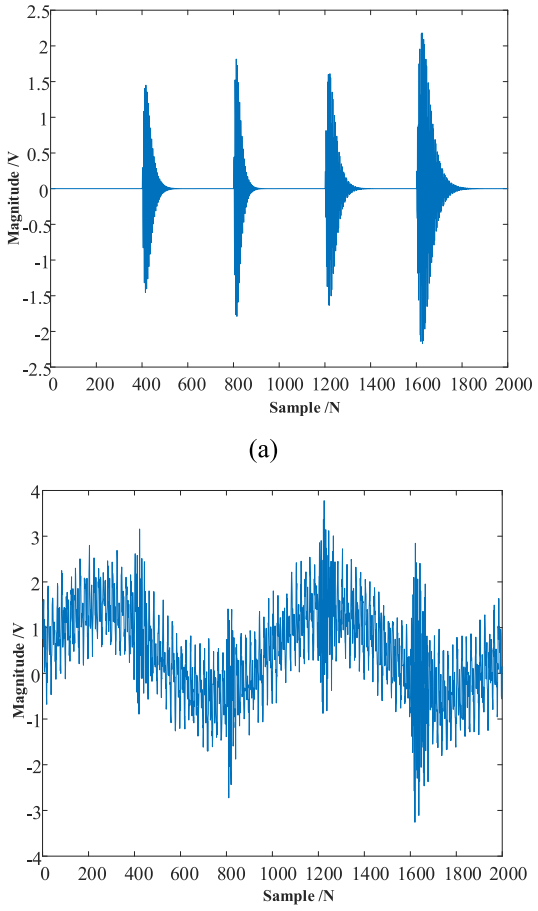

FIGURE 2. Simulating the original PD signal and the noise signal. (a) The analog PD signal. (b) The noise signal after adding the narrowband interference and the white noise.

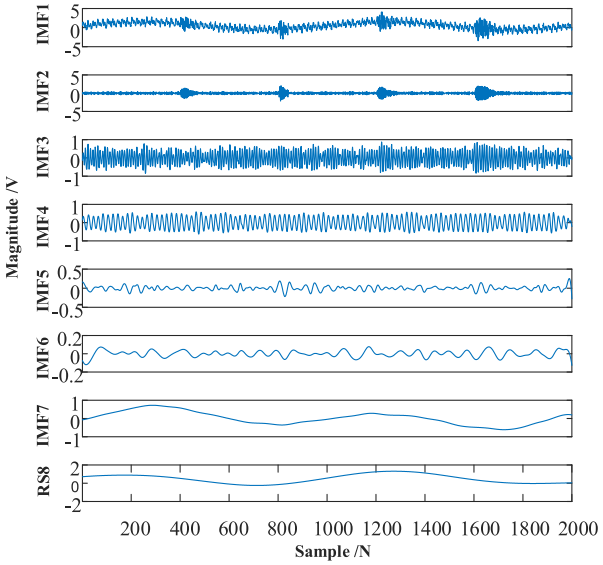

FIGURE 3. The NAEEMD decomposition of the modal function.

decomposition of the noise signal is performed to obtain the seven IMFs, of which RS8 is the signal margin, as shown in Fig.3.

As shown in in Fig.3, the PD signal fundamentally exists in the IMF1 and IMF2 modes and the white noise signal is mostly concentrated in the IMF3 mode. The IMF4∼IMF6 modes contain the narrowband periodic interference signals of different frequencies. IMF7 is clearly the false component of the decomposition, and it ought to be relinquished. It combines the energy density and the average period of the IMF correlation coefficient method when reconstructing the signal, so as to restore the true signal to the greatest extent. As appeared in Fig.3 the IMF transition is progressively natural, and the frequency components of different scales are clearly separated. Besides, the proposed NAEEMD method can separate the PD signal from the interference signal, and mitigate the modal aliasing phenomenon.

In order to validate the proposed method, the outcomes have been compared with the WAT denoising and EMD based threshold denoising for the analog noise discharge signal as shown in Fig.4.

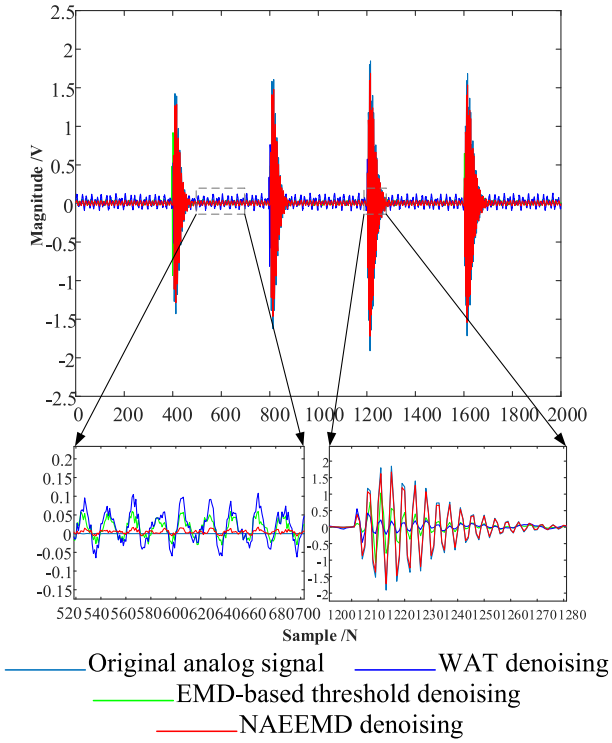

FIGURE 4. The simulated PD signal denoising results.

As seen in Fig.4, the waveform with the proposed NAEEMD denoising and the EMD-based threshold denoising are both closer to the original signal than with the WAT denoising. Moreover, both the noise suppression and the signal mutation characteristics are significantly better than the WAT denoising method. In additional, the simulation results showed that the waveform after NAEEMD denoising has more discharge information than the EMD-based threshold denoising waveform. That is because the margin obtained by the noise adaptive EEMD method after each decomposition does not rely on the independent decomposition after each noise addition. But it depends on the margin of the last decomposition, so that the reconstruction error is decreased and the signal has restored more realistically.

To evaluate the waveform characteristic after denoising, the signal-to-noise ratio (SNR), waveform correlation coefficient (NCC) and root mean square error (RMSE) are estimated as the following:

$$SNR = 10\lg \frac{\sum_{n=1}^{N} x(n)^2}{\sum_{n=1}^{N} [x(n) - \hat{x}(n)]^2} \tag{18}$$

$$NCC = \frac{\sum_{n=1}^{N} x(n)^* \hat{x}(n)}{\sqrt{(\sum_{n=1}^{N} x(n)^2)^* (\sum_{n=0}^{N} \hat{x}(n)^2)}} \tag{19}$$

$$RMSE = \sqrt{\frac{1}{N} \sum_{n=1}^{N} [x(n) - \hat{x}(n)]^2} \tag{20}$$

where $x(n)$ and $\hat{x}(n)$ are the time series of signals before noise reduction and after noise reduction, respectively.

The SNR value and the amplitude error are visibly measured by denoising. Furthermore, the larger SNR value, the smaller the amplitude error, which indicates better denoising effect. The waveform correlation coefficient is the microscopic measure of denoising effect. So that, the larger the waveform similarity coefficient indicates the smaller the waveform distortion and the better the denoising effect. The evaluation index values of the three denoising algorithms are shown in Table 2.

TABLE 2. Evaluation index values of three denoising algorithms.

Indicator / Method	*SNR*	*NCC*	*RMSE*
WAT denoising	15.1540	0.8557	0.4367
EMD-based threshold denoising	16.2365	0.8642	0.5253
NAEEMD denoising	18.8695	0.8865	0.1325

It can be seen from Table 2 that for the WAT denoising and EMD-based threshold denoising, although the latter's RMSE is higher than the former, both *SNR* and *NCC* are higher than the former. In general, the denoising effect with EMD-based threshold is better than WAT denoising. Concerning the proposed NAEEMD denoising, it can be seen that the three indicators are better than the EMD-based threshold denoising, it is further illustrated that the proposed method has acceptable advantages in PD denoising.

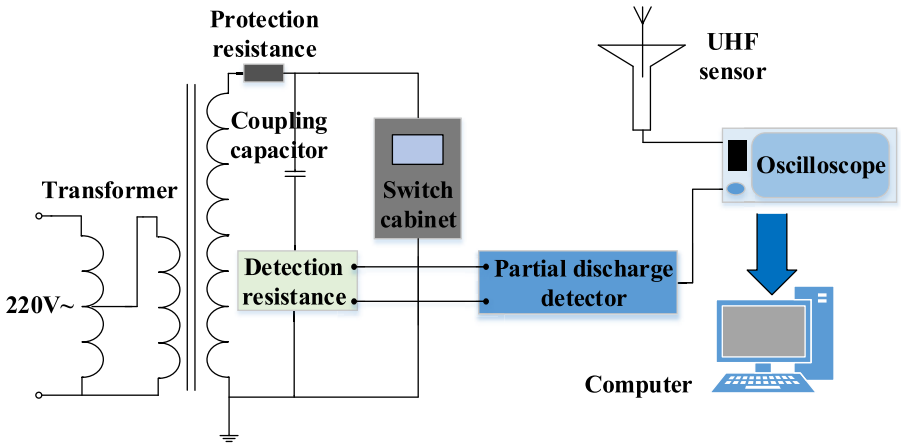

FIGURE 5. Wiring diagram of the switch cabinet PD experimental platform.

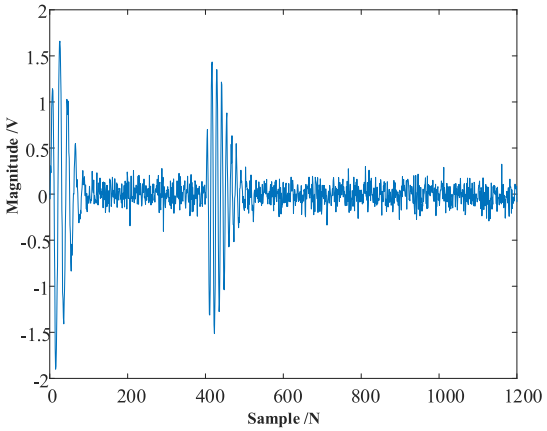

FIGURE 6. The switchgear noise-containing PD signal.

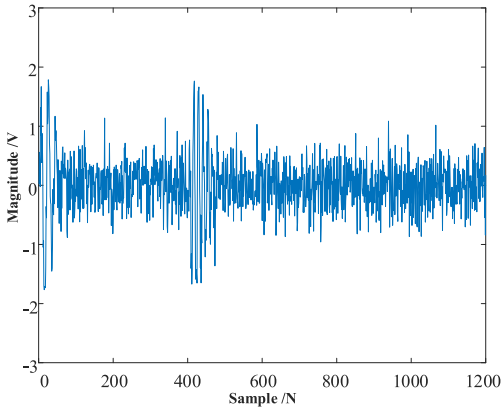

FIGURE 7. The processed PD signal.

IV. EXPERIMENTAL ANALYSIS

In order to verify the noise reduction effect of the proposed denoising method, a real switchgear PD signal is utilized in the laboratory, the switch cabinet PD experimental platform as shown in Fig.5.

The signal waveform is obtained by using an omnidirectional ultra-high frequency sensor and a high-speed digital storage oscilloscope. The omnidirectional antenna bandwidth is 0.2 $\sim$ 2GHz, and the oscilloscope sampling rate is 5GS/s. The discharge signal sampled at each power frequency cycle is taken as a sample.

The switchgear noise-containing PD signal is obtained through the laboratory simulation test, as shown in Fig.6. Due to the small degree of noise interference in the laboratory environment and to keep the test results closer to the actual switch cabinet PD signal, the PD signal obtained by the simulation test is processed as shown in Fig.7. In order to verify the effectiveness of the proposed NAEEMD denoising method for noise reduction, the WAT denoising and EMD-based threshold denoising are used to denoise the signal shown in Fig.7 as appeared in Fig.8. By comparing and analyzing the denoised signals of the three denoising methods, the characteristics of the three denoising methods are verified as the following.

It can be seen from Fig.8 that after utilizing the three methods of noise reduction, the noise interference of the PD signal that was originally submerged in the noise is effectively suppressed. Moreover, the noise-reduced signal maintains the contour of the original signal, which proves the feasibility and effectiveness of the three methods for denoising the PD signal. The WAT denoising and the EMD-based threshold denoising, Fig.8 (a) and (b) basically complete the denoising processing of the PD signal, however, a small portion of the original signal spectrum is lost and there is still some noise glitch after the denoising process. In Fig.8 (c), the proposed denoising method is succeeded to denoise the signal from the noise signal. In addition, the noise glitch of the signal is suppressed to a large extent, and the PD signal is almost completely extracted from the noise.

For further verifying the noise immunity of the proposed method, the spectrum analysis is performed on the measured original signal waveform and the latter has denoised by the three different methods, as shown in Fig.9. As shown in Fig.9, the useful information contained in the PD signal is mainly concentrated in the 0.5 MHz and 0.8 MHz

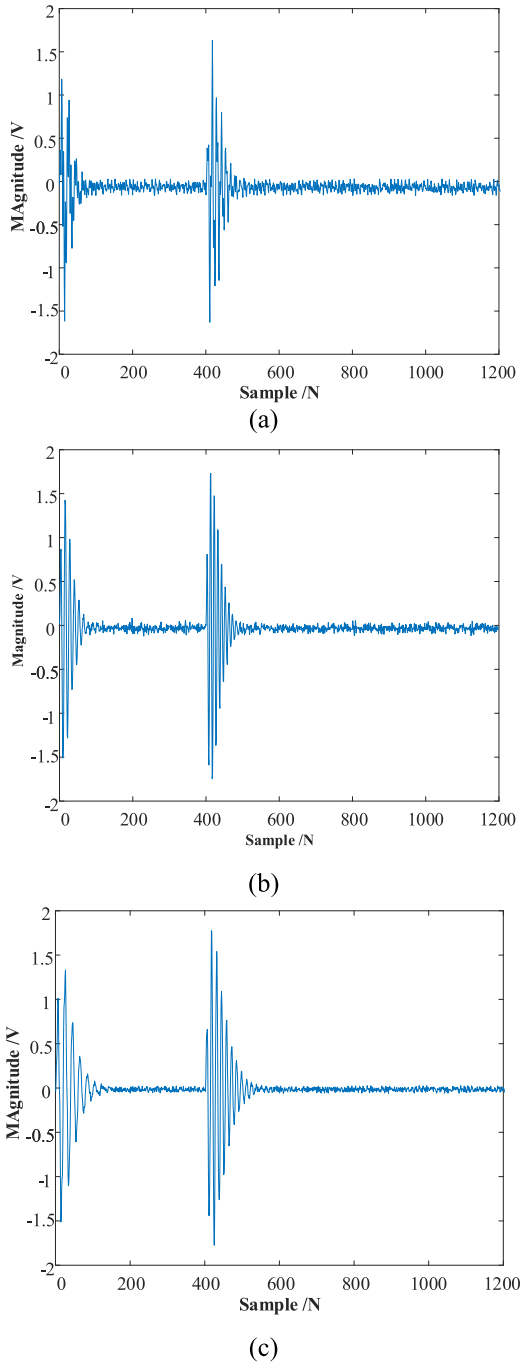

FIGURE 8. The result of denoising the measured PD signal. (a) The measured PD denoised signal of WAT denoising. (b) The measured PD denoised signal of EMD-based threshold denoising. (c) The measured PD denoised signal of NAEEMD denoising.

high frequency bands. Obviously, the narrowband interference signals are concentrated in the 0.2 MHz and 2 MHz frequency bands, while the remaining low frequency bands contain ambient noise information. Furthermore, with comparing the spectrum of the signal after denoising by the three methods with the spectrum of the measured original signal, it can be seen that the three denoising methods succeeded

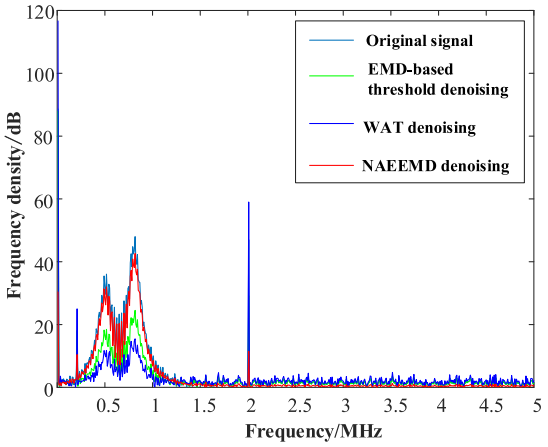

FIGURE 9. Spectrum analysis after denoising of measured PD signals.

in suppressing the narrowband interference signal of the PD signal and white noise denoising. Although, the EMD-based threshold denoising and the proposed denoising method are closer to the spectrum distribution of the original signal than the WAT denoising method. With further comparing the influence of narrowband interference and noise on the spectral distribution of the PD signal, it is obvious that the denoising waveform by proposed method is richer than the EMD-based threshold denoising method. Meanwhile, the signal spectrum after denoising with the proposed method is basically consistent with the spectrum waveform of the measured original signal, which embodies the superiority of the proposed method in the recognition and extraction of PD signal.

V. CONCLUSION

Aiming at the drawbacks of pattern aliasing in the conventional EMD decomposition and the lack of signal spectrum and reconstruction signal, this paper proposes a Novel Adaptive EEMD (NAEEMD) denoising method. The main idea of the proposed method is to decompose only the first-order mode after adding white noise to the original signal then adding the noise ceaselessly to the residual signal. The proposed method has been compared with the WAT denoising and EMD-based threshold denoising for validation. Based on the analysis and verification of the signal simulation and the actual example, it can be concluded that the NAEEMD method haven't the problem of selecting the basis function and number of decomposition layers compared with WAT denoising and EMD-based threshold denoising. Moreover, the proposed method completely denoises the signal characteristics and maintains the threshold denoising feature for each component in wavelet denoising. During the decomposition of the residual signal component by the proposed NAEEMD method, only the first-order mode is decomposed. Therefore, the margin isn't gotten by independent decomposition after each noise addition, but by the margin of the last decomposition. This largely reduces the reconstruction error after decomposition, which is not available in the

EMD-based threshold denoising and WAT denoising. In addition, it can be seen from the analysis of the PD signal that the proposed NAEEMD method is superior to the other two methods in terms of noise suppression and signal mutation characteristics.

REFERENCES

[1] H. Zheng, T. Zou, J. Hu, and H. Yu, "A framework for adaptive predictive control system based on zone control," *IEEE Access*, vol. 6, pp. 49513–49522, 2018.

[2] R. Moghaddass and J. Wang, "A hierarchical framework for smart grid anomaly detection using large-scale smart meter data," *IEEE Trans. Smart Grid*, vol. 9, no. 6, pp. 5820–5830, Nov. 2018.

[3] L. Luo, B. Han, J. Chen, G. Sheng, and X. Jiang, "Partial discharge detection and recognition in random matrix theory paradigm," *IEEE Access*, vol. 5, pp. 8205–8213, 2016.

[4] C. Boya, M. Ruiz-Llata, J. Posada, and J. A. Garcia-Souto, "Identification of multiple partial discharge sources using acoustic emission technique and blind source separation," *IEEE Trans. Dielectr. Electr. Insul.*, vol. 22, no. 3, pp. 1663–1673, Jun. 2015.

[5] L. Wei *et al.*, "A novel partial discharge ultra-high frequency signal de-noising method based on a single-channel blind source separation algorithm," *Energies*, vol. 11, no. 3, p. 509, 2018.

[6] Y. Chen, D. Wang, P. Liu, Z. Xu, C. Wei, and Q. Dong, "An improved approach of SFAP algorithm for suppressing concurrent narrowband and wideband interference," in *Proc. China Satell. Navigat. Conf. (CSNC)*. Singapore: Springer, vol. 2, 2016, pp. 69–80.

[7] G. Wang, S.-J. Kim, G.-S. Kil, and S.-W. Kim, "Optimization of wavelet and thresholding for partial discharge detection under HVDC," *IEEE Trans. Dielectr. Electr. Insul.*, vol. 24, no. 1, pp. 200–208, Feb. 2017.

[8] J. Li, C. Cheng, T. Jiang, and S. Grzybowski, "Wavelet de-noising of partial discharge signals based on genetic adaptive threshold estimation," *IEEE Trans. Dielectr. Electr. Insul.*, vol. 19, no. 2, pp. 543–549, Apr. 2012.

[9] Y. Luo, Z. Li, and H. Wang, "A review of online partial discharge measurement of large generators," *Energies*, vol. 10, no. 11, p. 1694, 2017.

[10] M. Mondal and G. B. Kumbhar, "Detection, measurement, and classification of partial discharge in a power transformer: Methods, trends, and future research," *IETE Tech. Rev.*, vol. 35, no. 5, pp. 483–493, 2018.

[11] I. Mitiche, G. Morison, A. Nesbitt, M. H. Narborough, P. Boreham, and B. G. Stewart, "An evaluation of total variation signal denoising methods for partial discharge signals," in *Proc. 13th Int. Elect. Insul. Conf. (INSUCON)*, May 2017, pp. 1–5.

[12] K. Ahmadi, A. Y. Javaid, and E. Salari, "An efficient compression scheme based on adaptive thresholding in wavelet domain using particle swarm optimization," *Signal Process., Image Commun.*, vol. 32, pp. 33–39, Mar. 2015.

[13] R. A. Hooshmand, M. Parastegari, and M. Yazdanpanah, "Simultaneous location of two partial discharge sources in power transformers based on acoustic emission using the modified binary partial swarm optimisation algorithm," *IET Sci., Meas. Technol.*, vol. 7, no. 2, pp. 119–127, 2013.

[14] Y. A. N. G. Kai, "Study method of signal processing in partial discharge," *Electrotech. Electric*, vol. 12, no. 10, pp. 14–25, 2014.

[15] K. Firuzi, M. Vakilian, B. T. Phung, and T. R. Blackburn, "Partial discharges pattern recognition of transformer defect model by LBP & HOG features," *IEEE Trans. Power Del.*, vol. 34, no. 2, pp. 542–550, Apr. 2019.

[16] N. A. Yusoff *et al.*, "Denoising technique for partial discharge signal: A comparison performance between artificial neural network, fast Fourier transform and discrete wavelet transform," in *Proc. IEEE Int. Conf. Power Energy (PECon)*, Nov. 2016, pp. 311–316.

[17] R. Hussein, K. B. Shaban, and A. H. El-Hag, "Energy conservation-based thresholding for effective wavelet denoising of partial discharge signals," *IET Sci., Meas. Technol.*, vol. 10, no. 7, pp. 813–822 2016.

[18] X. Li *et al.*, "Comparison of different time-frequency analysis methods for sparse representation of PD-induced UHF signal," in *Proc. China Int. Conf. Electr. Distrib. (CICED)*, Aug. 2015, pp. 1–5.

[19] N. Jmail, M. Zaghdoud, A. Hadriche, T. Frikha, C. B. Amar, and C. Bénar, "Integration of stationary wavelet transform on a dynamic partial reconfiguration for recognition of pre-ictal gamma oscillations," *Heliyon*, vol. 4, no. 2, 2018, Art. no. e00530.

[20] H. Wang, C.-J. Huang, L.-P. Yao, W.-D. Zheng, Y. Qian, and X. C. Jiang, "Application of reassigned cohen class time-frequency distribution to the analysis of acoustic emission partial discharge signal for GIS," *Gaodianya-Jishu/ High Voltage Eng.*, vol. 36, no. 11, pp. 2724–2730, 2010.

[21] T. Liu, S. Yan, and W. Zhang, "Time–frequency analysis of nonstationary vibration signals for deployable structures by using the constant-Q nonstationary Gabor transform," *Mech. Syst. Signal Process.*, vol. 75, pp. 228–244, Jun. 2016.

[22] M. Parchami, W.-P. Zhu, B. Champagne, and E. Plourde, "Recent developments in speech enhancement in the short-time Fourier transform domain," *IEEE Circuits Syst. Mag.*, vol. 16, no. 3, pp. 45–77, 3rd Quart., 2016.

[23] W. Jenkal, R. Latif, A. Toumanari, A. Dliou, B. El B'Charri, and F. M. R. Maoulainine "An efficient algorithm of ECG signal denoising using the adaptive dual threshold filter and the discrete wavelet transform," *Biocybern. Biomed. Eng.*, vol. 36, no. 3, pp. 499–508, 2016.

[24] M. Kedadouche, M. Thomas, and A. Tahan, "A comparative study between empirical wavelet transforms and empirical mode decomposition methods: Application to bearing defect diagnosis," *Mech. Syst. Signal Process.*, vol. 81, pp. 88–107, Dec. 2016.

[25] S. Roostaee, M. S. Thomas, and S. Mehfuz, "Experimental studies on impedance based fault location for long transmission lines," *Protection Control Mod. Power Syst.*, vol. 2, no. 1, p. 16, 2017.

[26] R. Jia, Q. Xu, L. Tian, H. Li, and W. Liu, "Denoising of partial discharge based on empirical mode decomposition and intrinsic mode function reconstruction," *Trans. China Electrotech. Soc.*, vol. 23, no. 1, pp. 13–18, Jan. 2008.

[27] B. Zhu, S. Ma, R. Xie, J. Chevallier, and Y.-M. Wei, "Hilbert spectra and empirical mode decomposition: A multiscale event analysis method to detect the impact of economic crises on the European carbon market," *Comput. Econ.*, vol. 52, pp. 105–121, Jun. 2018.

[28] P. Ray, A. K. Maitra, and A. Basuray, "A new threshold function for de-noising partial discharge signal based on wavelet transform," in *Proc. Int. Conf. Signal Process., Image Process. Pattern Recognit.*, Feb. 2013, pp. 185–189.

[29] T. Rajaee and H. Jafari, "Utilization of WGEP and WDT models by wavelet denoising to predict water quality parameters in rivers," *J. Hydrol. Eng.*, vol. 23, no. 12, 2018, Art. no. 04018054.

[30] H. Han, S. Cho, S. Kwon, and S.-B. Cho, "Fault diagnosis using improved complete ensemble empirical mode decomposition with adaptive noise and power-based intrinsic mode function selection algorithm," *Electronics*, vol. 7, no. 2, p. 16, 2018.

[31] D. Chen, J. Lin, and Y. Li, "Modified complementary ensemble empirical mode decomposition and intrinsic mode functions evaluation index for high-speed train gearbox fault diagnosis," *J. Sound Vib.*, vol. 424, pp. 192–207, Jun. 2018.

[32] Y. Lv, R. Yuan, and G. Song, "Multivariate empirical mode decomposition and its application to fault diagnosis of rolling bearing," *Mech. Syst. Signal Process.*, vol. 81, pp. 219–234, Dec. 2016.

[33] G. R. Naik, S. E. Selvan, and H. T. Nguyen, "Single-channel EMG classification with ensemble-empirical-mode-decomposition-based ICA for diagnosing neuromuscular disorders," *IEEE Trans. Neural Syst. Rehabil. Eng.*, vol. 24, no. 7, pp. 734–743, Jul. 2016.

[34] S. Lahmiri, "Comparing variational and empirical mode decomposition in forecasting day-ahead energy prices," *IEEE Syst. J.*, vol. 11, no. 3, pp. 1907–1910, Sep. 2017.

[35] A. Jahan, K. L. Edwards, and M. Bahraminasab, *Multi-criteria Decision Analysis for Supporting the Selection of Engineering Materials in Product Design*. Oxford, U.K.: Butterworth-Heinemann, 2016.

[36] D. H. Pandya, S. H. Upadhyay, and S. P. Harsha, "Fault diagnosis of rolling element bearing with intrinsic mode function of acoustic emission data using APF-KNN," *Expert Syst. Appl.*, vol. 40, no. 10, pp. 4137–4145, 2013.

[37] Z. Wu and N. E. Huang, "A study of the characteristics of white noise using the empirical mode decomposition method," *Proc. R. Soc. Lond. A, Math., Phys. Eng. Sci.*, vol. 460, no. 2046, pp. 1597–1611, 2004.

[38] N. Nava, T. Di Matteo, and T. Aste, "Dynamic correlations at different time-scales with empirical mode decomposition," *Phys. A, Stat. Mech. Appl.*, vol. 502, pp. 534–544, Jul. 2018.

[39] A. Kucyi, J. Schrouff, S. Bickel, B. L. Foster, J. M. Shine, and J. Parvizi, "Intracranial electrophysiology reveals reproducible intrinsic functional connectivity within human brain networks," *J. Neurosci.*, vol. 38, no. 17, pp. 4230–4242, 2018.
[40] A. R. Mor, L. C. C. Heredia, D. A. Harmsen, and F. A. Muñoz, "A new design of a test platform for testing multiple partial discharge sources," *Int. J. Elect. Power Energy Syst.*, vol. 94, pp. 374–384, Jan. 2018.

TAO JIN (M'08) was born in Hubei, China, in 1976. He received the B.S. and M.S. degrees from Yanshan University, in 1998 and 2001, respectively, and the Ph.D. degree in electrical engineering from Shanghai Jiao Tong University, in 2005, where he was a Postdoctoral Researcher, from 2005 to 2007. During this time, he was in charge of a research group in the biggest dry-type transformer company in Asia, Sunten Electrical Co., Ltd, to develop new transformer technology for distribution grids. From 2008 to 2009, he was a Research Scientist with Virginia Tech, Blacksburg, USA, where he was involved in the design and testing of PMU technology and GPS/internet-based power system frequency monitoring networks. In 2010, he joined Imperial College London, U.K., as a European Union Marie Curie Research Fellow, where he was focused on electrical technologies related to smart grids. He is currently a Professor with the College of Electrical Engineering & Automation, Fuzhou University, China.

Prof. Jin has published about 110 papers. He is a member of the IEEE Power and Energy Society and the IEEE Industrial Electronics Society. He is also a special committee member of the Chinese Society of Electrical Engineering, the China Electrotechnical Society, and more. He currently serves as an Associate Editor for the *China Measurement & Testing Technology* and other journals.

QIANGGUANG LI was born in Jiangxi, China, in 1994. He received the B.S. degree from the Nanchang University College of Science and Technology, in 2017. He is currently pursuing the M.S. degree with the School of Electrical Engineering and Automation, Fuzhou University. His current research interests include on-line fault monitoring and protection of switchgear.

MOHAMED A. MOHAMED was born in Minia, Egypt, in 1985. He received the B.Sc. and M.Sc. degrees from Minia University, Minia, in 2006 and 2010, respectively, and the Ph.D. degree from King Saud University, Riyadh, Saudi Arabia, in 2016. He joined the College of Electrical Engineering & Automation, Fuzhou University, China, as a Postdoctoral Research Fellow, in 2018. He has been a Faculty Member with the Department of Electrical Engineering, College of Engineering, Minia University, since 2008. He has supervised multiple M.Sc. and Ph.D. theses, worked on a number of technical projects, and published various papers and books@perio. His current research interests include renewable energy, energy management, power electronics, power quality, optimization, and smart grids. He has also joined the editorial board of some scientific journals and the steering committees of many international conferences.